

NASA/TM—2002-211481



# Thermal Conductivity and Sintering Behavior of Advanced Thermal Barrier Coatings

Dongming Zhu  
Ohio Aerospace Institute, Brook Park, Ohio

Robert A. Miller  
Glenn Research Center, Cleveland, Ohio

Prepared for the  
26th Annual International Conference on Advanced Ceramics and Composites  
sponsored by the American Ceramics Society  
Cocoa Beach, Florida, January 13–18, 2002

National Aeronautics and  
Space Administration

Glenn Research Center

---

May 2002

## Acknowledgments

This work was supported by NASA Ultra-Efficient Engine Technology (UEET) Program. The authors gratefully acknowledge the help of our colleagues at NASA Glenn Research Center, especially, Narottam Bansal for hot-processed specimen processing, Jeffrey I. Eldridge for emittance measurements, James A. Nesbitt for cyclic furnace testing and XRF compositional analysis of the new coating materials. The authors are also grateful to George W. Leissler, QSS Group, Inc. at the NASA Glenn Research Center, for his assistance in the preparation of plasma-sprayed thermal barrier coatings, Robert W. Bruce, General Electric Aircraft Engines, and Kenneth S. Murphy, Howmet Research Corporation, for EB-PVD coating processing.

Available from

NASA Center for Aerospace Information  
7121 Standard Drive  
Hanover, MD 21076

National Technical Information Service  
5285 Port Royal Road  
Springfield, VA 22100

Available electronically at <http://gltrs.grc.nasa.gov/GLTRS>

# THERMAL CONDUCTIVITY AND SINTERING BEHAVIOR OF ADVANCED THERMAL BARRIER COATINGS

Dongming Zhu  
Ohio Aerospace Institute  
Brook Park, Ohio 44142

Robert A. Miller  
National Aeronautics and Space Administration  
Glenn Research Center  
Cleveland, Ohio 44135

## ABSTRACT

Advanced thermal barrier coatings, having significantly reduced long-term thermal conductivities, are being developed using an approach that emphasizes real-time monitoring of thermal conductivity under conditions that are engine-like in terms of temperatures and heat fluxes. This is in contrast to the traditional approach where coatings are initially optimized in terms of furnace and burner rig durability with subsequent measurement in the as-processed or furnace-sintered condition. The present work establishes a laser high-heat-flux test as the basis for evaluating advanced plasma-sprayed and physical vapor-deposited thermal barrier coatings under the NASA Ultra Efficient Engine Technology (UEET) Program. The candidate coating materials for this program are novel thermal barrier coatings that are found to have significantly reduced thermal conductivities due to an oxide-defect-cluster design. Critical issues for designing advanced low conductivity coatings with improved coating durability are also discussed.

## INTRODUCTION

Ceramic thermal barrier coatings (TBCs) are receiving increased attention for advanced gas turbine engine applications. The thermal barrier coatings are considered technologically important because of their ability to further increase engine operating temperatures, and to achieve engine efficiency, emission and performance goals. In order to fully take advantage of the TBC capability, an aggressive design approach—allowing greater temperature reductions through the coating systems and less cooling air to the components—is required whenever possible. Advanced thermal barrier coatings that have significantly lower thermal conductivity and better thermal stability than current coatings must be developed for future ultra efficient, low emission engine systems.

Higher surface temperatures and larger thermal gradients are expected in advanced thermal barrier coating systems as compared to conventional coating systems. As illustrated in Fig. 1, thermal barrier coatings with lower thermal conductivity can be used in thin coating configurations while still achieving sufficient temperature reductions at higher engine operating temperatures. The low conductivity coatings will have a significant advantage over the conventional ones particularly for rotating engine components (such as turbine blades), where a reduced weight is highly desirable.

The development of low conductivity thermal barrier coatings requires test techniques that can accurately and effectively evaluate coating thermal conductivity at high surface temperatures (typically at 1300 to 1400°C). It is known that the coating thermal conductivity can increase significantly due to coating sintering and/or phase structure changes after a long-term thermal exposure. Therefore, the evaluations of the coating initial and after-exposure thermal conductivities, and of the conductivity rate of increase are crucial in characterizing the coating's performance. In this study, a laser high-heat-flux test technique is established for evaluating advanced plasma-sprayed and electron-beam physical vapor-deposited thermal barrier coatings under the NASA Ultra Efficient Engine Technology (UEET) program. The test approach emphasizes real-time monitoring of thermal conductivity (and, therefore, the conductivity increases) at high temperature under simulated engine thermal gradients to determine the optimum coating compositions. Novel candidate coating materials are developed using an oxide defect clustering concept that incorporates paired cluster dopants into zirconia-ytria or hafnia-ytria systems, thereby achieving low thermal conductivity and sintering resistant coatings. The coating durability issues and the dopant effect on coating furnace cyclic behavior are also discussed in this paper.

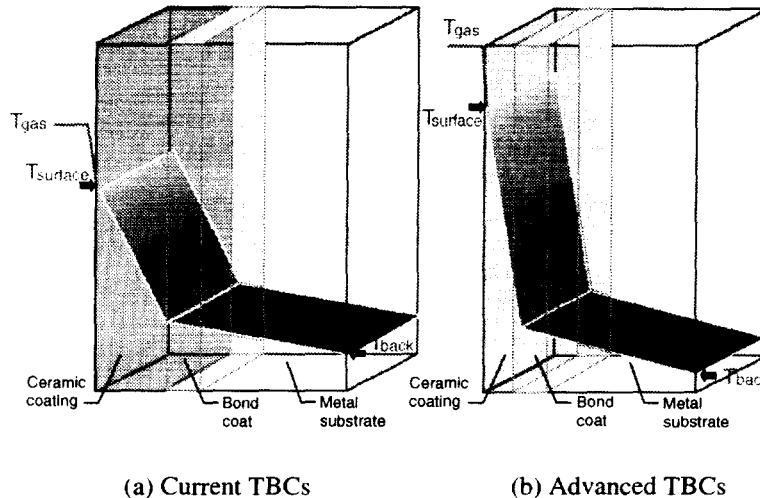


Fig. 1 Advanced thermal barrier coatings with lower thermal conductivity and better temperature stability will allow the use of a thinner coating system to achieve a larger temperature reduction at higher engine operating temperatures. The substrate temperature can be maintained at a lower level while the cooling can be significantly reduced. A thin coating system is highly desirable for engine rotating components such as airfoils where a reduced weight is critical.

## EXPERIMENTAL MATERIALS AND METHODS

### ADVANCED DEFECT-CLUSTERING OXIDE THERMAL BARRIER COATINGS

Advanced oxide thermal barrier coatings were developed using a multi-component defect-clustering approach [1, 2]. In this approach, the advanced oxide coatings were designed by incorporating multi-component, paired-cluster oxide dopants into conventional zirconia- and hafnia-yttria oxides. The dopant oxides were selected by considering their interatomic and chemical potentials, lattice elastic strain energy (ionic size effect), polarization as well as electro-neutrality within the oxides. The added dopant oxides were intended to effectively promote the creation of thermodynamically stable, highly defective lattice structures with essentially immobile defect clusters and/or nanoscale ordered phases, thus reducing oxide coating thermal conductivity and improving coating sintering resistance.

In the present study, examples of selected clustered oxide thermal barrier coating systems including  $ZrO_2$ - $Y_2O_3$ - $Nd_2O_3$ ( $Gd_2O_3$ , $Sm_2O_3$ )- $Yb_2O_3$ ( $Sc_2O_3$ ) [2] were given, and their conductivity and sintering behavior was investigated. Emphasis was placed on the effect of total dopant concentrations on the coating thermal conductivity, sintering resistance, and durability. The advanced thermal barrier coating systems, typically consisting of a 180 to 250  $\mu m$  the ceramic top coat and a 75 to 120  $\mu m$  NiCrAlY or NiAl intermediate bond coat, were either plasma-sprayed or electron-beam physical vapor deposited on to the 25.4 mm diameter and 3.2 mm thick Rene N5 disk substrates. The plasma-sprayed coatings were processed using pre-alloyed powders. The ceramic powders with designed compositions were first spray-dried, then plasma-reacted and spheroidized, and finally plasma-sprayed into the coating form. The advanced EB-PVD coatings were deposited using pre-fabricated evaporation ingots that were made of the carefully designed compositions. The EB-PVD coatings were processed into test coating specimens by two different vendors (General Electric Aircraft Engines, Cincinnati, Ohio and Howmet Coatings Corporation, Whitehall, Michigan).

## LASER TEST APPROACH FOR EVALUATING ADVANCED THERMAL BARRIER COATINGS

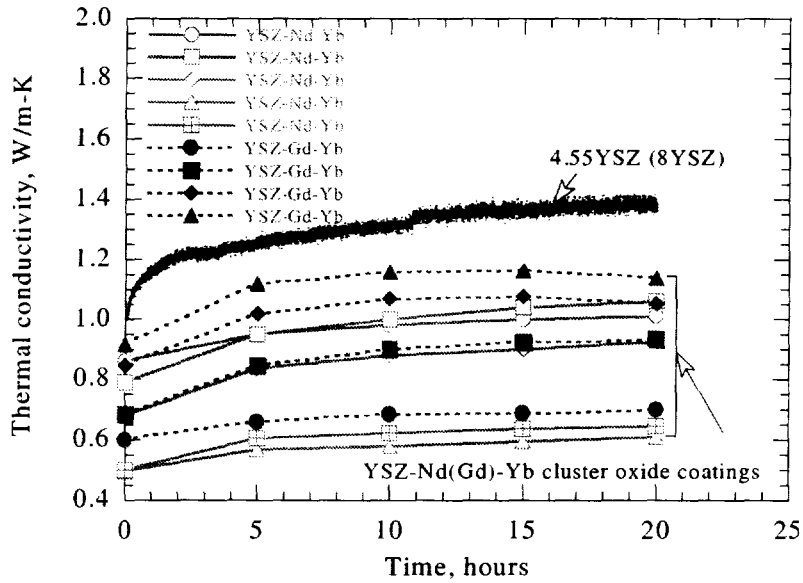
A 3.0 kW CO<sub>2</sub> laser (wavelength 10.6  $\mu\text{m}$ ) high heat flux thermal conductivity rig was established for evaluating advanced thermal barrier coatings. The general approaches for coating conductivity measurement under the high temperature and high thermal gradient conditions have been described in detail elsewhere [3-5]. In this study, a 25.4 mm diameter disk specimen configuration was used. During the testing, a large thermal gradient in the ceramic coating can be established by the laser surface heating and backside air-cooling. A given constant laser-delivered heat flux was applied to the coating surface throughout a standard 20 hr steady-state test period. Thermal conductivity of each candidate ceramic coating was determined in real-time during the 20 hr laser test, based on the applied laser heat flux and the measured temperature gradient across the coating. The surface temperature for all test specimens was at 1316°C at the beginning of the tests. The coating/metal interface temperature was approximately in the range of 950 to 1100°C, depending on the coating thermal conductivity and applied laser heat flux. Since the coating conductivity increases with time due to ceramic sintering, the coating surface temperature will continuously drop under the fixed laser heat flux condition. The measured initial coating conductivity ( $k_0$ ), the conductivity at 20 hrs ( $k_{20}$ ), and the conductivity rate of increase were used for evaluating the candidate coating performance. It should be mentioned that for some of the EB-PVD oxide coating systems, the coating conductivity after 5 hrs testing ( $k_5$ ) was used for characterizing the coating behavior. This is a viable approach for effectively reducing the testing time, because the EB-PVD coatings usually reached a steady-state conductivity increase stage after 5 hrs of testing, with a relatively low subsequent rate of conductivity increase.

## EXPERIMENTAL RESULTS

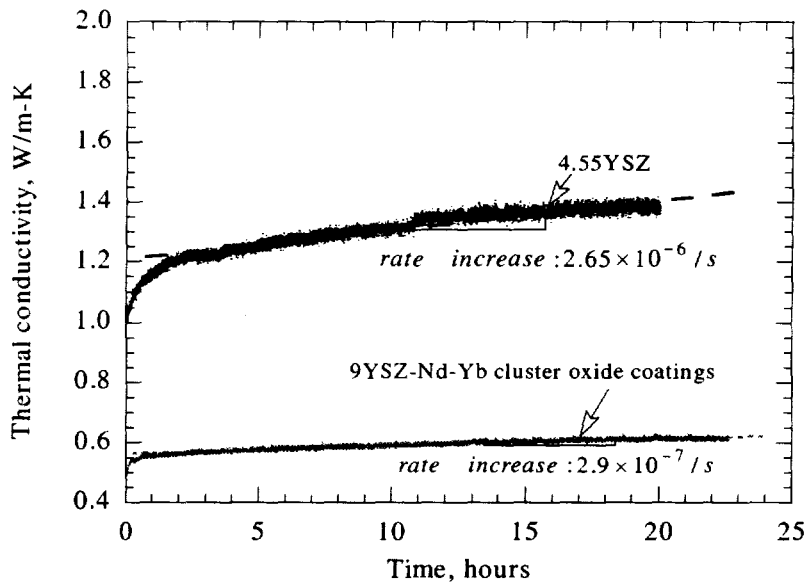
### THERMAL CONDUCTIVITY OF ADVANCED THERMAL BARRIER COATINGS

Figure 2 illustrates high temperature thermal conductivity of plasma-sprayed oxide cluster thermal barrier coatings as a function of test time. These advanced oxide coatings investigated in this study consisted primarily of ZrO<sub>2</sub>-Y<sub>2</sub>O<sub>3</sub>, but were also co-doped with additional paired rare earth oxides Nd<sub>2</sub>O<sub>3</sub>-Yb<sub>2</sub>O<sub>3</sub> or Gd<sub>2</sub>O<sub>3</sub>-Yb<sub>2</sub>O<sub>3</sub> (i.e., YSZ-Nd-Yb and YSZ-Gd-Yb oxide systems). As a comparison, the thermal conductivity of a baseline coating, ZrO<sub>2</sub>-4.55mol%Y<sub>2</sub>O<sub>3</sub> (i.e., ZrO<sub>2</sub>-8wt%Y<sub>2</sub>O<sub>3</sub>, or 8YSZ), is also plotted in Fig. 2. It can be seen that the coating conductivity generally increased with time. The advanced cluster oxide coating systems exhibited much lower thermal conductivity and conductivity increases than the conventional baseline coating. As shown in Fig. 2 (a), approximately one third of the 20-hr baseline coating conductivity value was achieved for some of best coating systems after the 20 hr laser high temperature tests. Figure 2(b) shows that the 9YSZ-Nd-Yb coating (which contains 9 mol%Y<sub>2</sub>O<sub>3</sub> stabilizer plus some additional dopant cluster oxides Nd<sub>2</sub>O<sub>3</sub> and Yb<sub>2</sub>O<sub>3</sub>) achieved almost one order-of-magnitude lower conductivity rate of increase as compared to the ZrO<sub>2</sub>-4.55mol%Y<sub>2</sub>O<sub>3</sub> baseline coating.

Figure 3 shows thermal conductivity and the rate of conductivity increase, of various plasma-sprayed cluster oxide thermal barrier coatings as a function of total dopant concentration. Figure 3 (a) illustrates the initial and 20-hr conductivity values of the coatings. It can be seen that the baseline 4.55YSZ coating had an initial conductivity of about 1.0 W/m-K. The conductivity of the baseline coating increased to about 1.4 W/m-K after 20 hours of high-heat-flux testing. In contrast, the oxide cluster coatings, including YSZ-Nd-Yb, YSZ-Gd-Yb and YSZ-Sm-Yb systems, exhibited lower initial and 20-hr thermal conductivities than the baseline coating. Thermal conductivity of the cluster oxide coatings generally decreased with increasing total dopant concentration. However, a very low conductivity region was observed in the concentration range that contains 6-13 mol% of the total dopants. Similar behavior was observed for the rate of conductivity increase data, shown in Fig. 3 (b). A minimum region for the rate of increase was also observed in the dopant concentration range of 6-13 mol%, corresponding well with the low conductivity valley region for the conductivity of the coating systems.



(a)



(b)

Fig. 2. Thermal conductivity of plasma-sprayed oxide cluster thermal barrier coatings and a baseline  $ZrO_2$ -4.55mol% $Y_2O_3$  (4.55YSZ) coating as a function of test time, determined using a laser steady-state heat flux technique at a surface temperature of 1316°C. (a) Thermal conductivity of various YSZ-Nd-Yb and YSZ-Gd-Yb oxide coating systems showing low conductivity was achieved for the advanced cluster oxide coatings. (b) Thermal conductivity rates of increase for the 9YSZ-Nd-Yb and baseline 4.55YSZ coating showing significantly reduced conductivity rises for the advanced coating as compared to the baseline coating after the 20 hr laser testing.

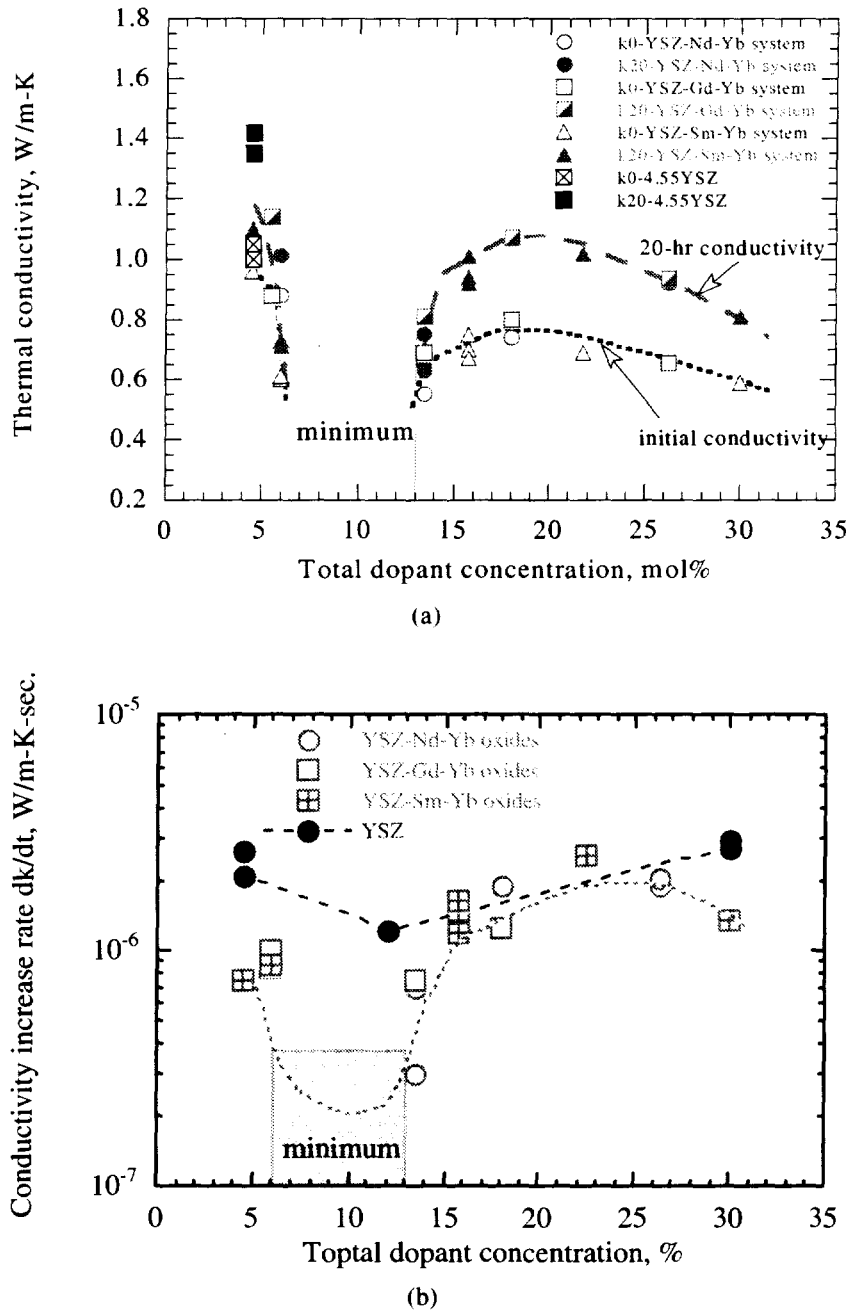


Fig. 3 Thermal conductivity, and the conductivity rate of increase, of various plasma-sprayed cluster oxide thermal barrier coatings as a function of total dopant concentration, determined by using a laser heat flux technique at the surface temperature of 1316°C. (a) Initial and 20 hr thermal conductivity values of 4.55YSZ, and the oxide coatings YSZ co-doped with  $\text{Nd}_2\text{O}_3\text{-Yb}_2\text{O}_3$ ,  $\text{Gd}_2\text{O}_3\text{-Yb}_2\text{O}_3$ , or  $\text{Sm}_2\text{O}_3\text{-Yb}_2\text{O}_3$ . A low conductivity regime is observed for the coatings in the range of 6 to 15 mol% total dopant concentration. (b) Corresponding conductivity rate of increase as a function of total dopant concentration, also showing a low rate regime in the range of 6 to 13 mol% total dopant concentration.

In order to investigate the effect of the cluster dopant concentration ratio on conductivity, plasma-sprayed  $ZrO_2$ - $Y_2O_3$ - $Nd_2O_3$ - $Yb_2O_3$  oxide coatings with decoupled cluster dopant concentrations were designed and prepared near the optimum low conductivity region. This set of oxide coatings had compositions ranging from YSZ only, YSZ plus a single  $Nd_2O_3$  or  $Yb_2O_3$  dopant, YSZ plus both the  $Nd_2O_3$  or  $Yb_2O_3$  but in varying the relative concentrations (with either equal or non-equal cluster dopant concentrations). Figure 4 shows the thermal conductivity results of the YSZ-Nd-Yb oxide thermal barrier coatings as a function of total dopant concentration and cluster dopant concentration ratio (ratio of  $Yb_2O_3$  to  $Nd_2O_3$  in mol%). It can be seen that thermal barrier coatings of  $ZrO_2$ - $Y_2O_3$ , and  $ZrO_2$ - $Y_2O_3$  with a single cluster dopant, Nd or Yb, showed typically higher thermal conductivities than the coatings of  $ZrO_2$ - $Y_2O_3$  with paired dopant additions ( $Nd_2O_3$ + $Yb_2O_3$ ). The cluster oxide coatings with equal amount of cluster dopants added ( $Yb_2O_3/Nd_2O_3 = 1$ ) often showed the lowest conductivity at a given total dopant concentrations. The paired dopants (with equal cluster dopant concentrations) especially showed significant beneficial effects in reducing the coating conductivity at about 10 mol% dopant concentrations.

Thermal conductivity of electron-beam physical vapor-deposited (EB-PVD) cluster oxide thermal barrier coatings was also investigated using the laser heat flux technique. Figure 5 shows typical conductivity changes as a function of time for EB-PVD processed  $ZrO_2$ -(4~6 mol%)  $Y_2O_3$ -Nd-Yb cluster oxide coatings. It can be seen that the cluster oxide coatings exhibited lower thermal conductivities and the rates of conductivity increase compared to the baseline  $ZrO_2$ -4.55%mol $Y_2O_3$  coating. The conductivity for the clustered coatings can be as low as 0.85 W/m-K after the 20 hr high temperature testing, as compared to the conductivity of 1.85 to 1.90 W/m-K for the baseline coating. The conductivity rate of increase was also reduced to  $0.8 \times 10^{-6} \sim 1.0 \times 10^{-6}$  W/m-K-s from the baseline coating value of  $1.3 \times 10^{-6}$  W/m-K-s by the addition of the cluster dopants.

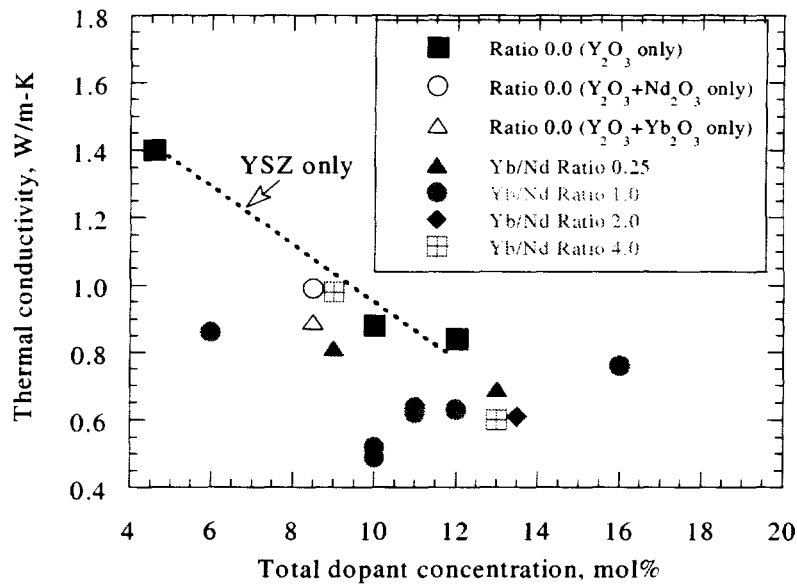


Fig. 4 Thermal conductivity of plasma-sprayed  $ZrO_2$ - $Y_2O_3$ - $Nd_2O_3$ - $Yb_2O_3$  cluster oxide thermal barrier coatings as a function of total dopant concentration and cluster dopant concentration ratio of  $Yb_2O_3$  to  $Nd_2O_3$  (in mol%) near the optimum low conductivity region. The cluster oxide coatings with the equal cluster oxide dopants ( $Yb_2O_3/Nd_2O_3 = 1$  in mol%) showed the lowest conductivity at 10 mol% total dopant concentration.



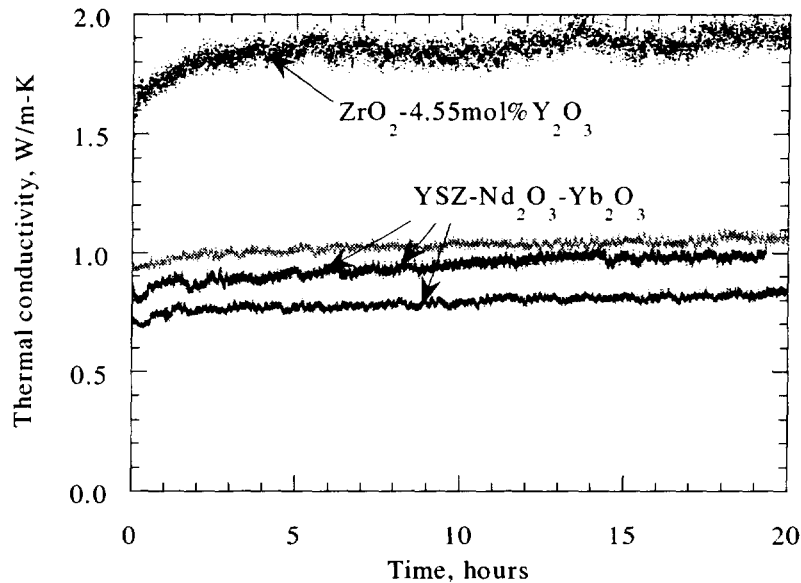


Fig. 5 Thermal conductivity of EB-PVD processed  $ZrO_2$ -(4~6mol%) $Y_2O_3$ -Nd-Yb cluster oxide thermal barrier coatings as a function of time. The oxide coatings exhibited significantly lower thermal conductivity and conductivity rate of increase than the baseline  $ZrO_2$ -4.55mol% $Y_2O_3$  coating.

Figure 6 illustrates thermal conductivity of various cluster oxide thermal barrier coatings as a function of total dopant concentration after 5 hr or 20 hr laser high heat flux tests at 1316°C. The conductivity data were plotted for selected NASA composition cluster oxide coatings that were prepared at General Electric Aircraft Engines Company and Howmet Coatings Corporation. Note that for some coating systems, the 5-hr conductivity data  $k_5$  (instead of 20-hr conductivity data  $k_{20}$ ) were used. This is still an acceptable approach based on the considerations that there is only small differences between  $k_5$  and  $k_{20}$  for the cluster EB-PVD coatings, simply because the coatings have reached a steady-state conductivity increase stage and also have relatively low rates of conductivity increase. It can be seen that the EB-PVD coating systems generally showed lower thermal conductivity than the YSZ coatings at any given total dopant concentration. In addition, similar to the plasma-sprayed coatings, the EB-PVD coating systems also exhibited a low conductivity region which is centered around 10 mol % total dopant concentration.

#### FURNACE CYCLIC BEHAVIOR OF THE ADVANCED THERMAL BARRIER COATINGS

Furnace cyclic tests have been carried out to evaluate durability of the advanced oxide coating systems. The coating specimens were thermal cyclic tested at 1160°C using a tubular or a box furnace with 45 min hot time cycles [6]. Figure 7 summarizes the test results for various coating compositions which were processed from different batches. It can be seen that, regardless the relatively large scatter, the coating cyclic life generally decreased with increasing the total dopant concentration. The cluster oxide coatings followed a similar trend as compared to the yttria-zirconia (YSZ only) coatings in the furnace cyclic behavior. However, the present results suggest some beneficial effect in improving coating cyclic lives by the addition of cluster oxide dopants. The multi-component cluster oxide coatings typically showed better cyclic lives than only yttria-doped zirconia coatings at given dopant concentrations. In fact, within the optimum low conductivity region of 6 to 13 mol% dopant concentration, significant coating life improvements (in some cases, coating lives comparable to those of zirconia-4.55 mol%yttria) have been observed for the initial processed (no processing optimization) cluster oxide coatings as compared to the YSZ coatings. Moderate coating life increases were also observed by coating composition, microstructure and bond coat modifications [6]. Further life improvements will be expected by utilizing advanced coatings architecture design, dopant type and composition optimization, and improved processing techniques.

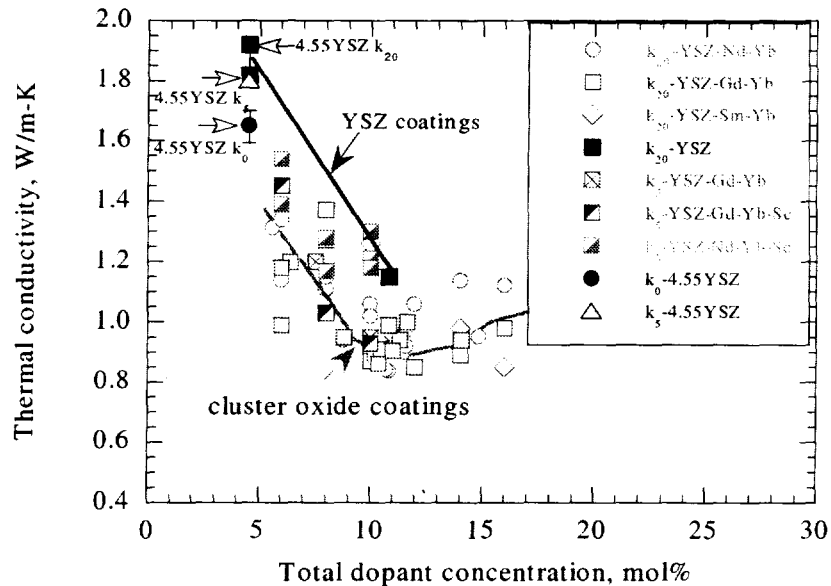


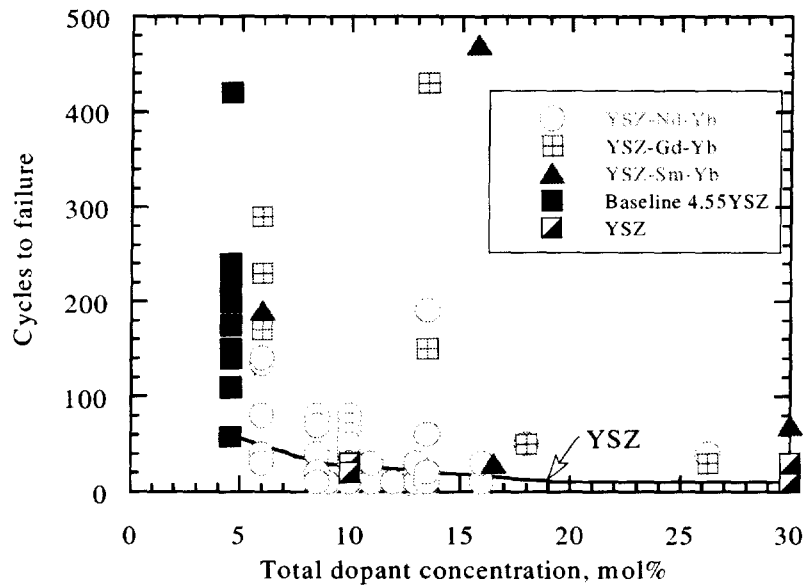
Fig. 6 Thermal conductivity of various electron-beam physical-vapor-deposited (EB-PVD) cluster oxide thermal barrier coatings as a function of total dopant concentration. The data are compiled with various NASA composition cluster oxide coatings that were prepared at General Electric Aircraft Engines company and Howmet Coatings Corporation. Similar to the plasma-sprayed coatings, the EB-PVD coating systems also showed a low conductivity region at about 10 mol % total dopant concentration.

### DISCUSSION

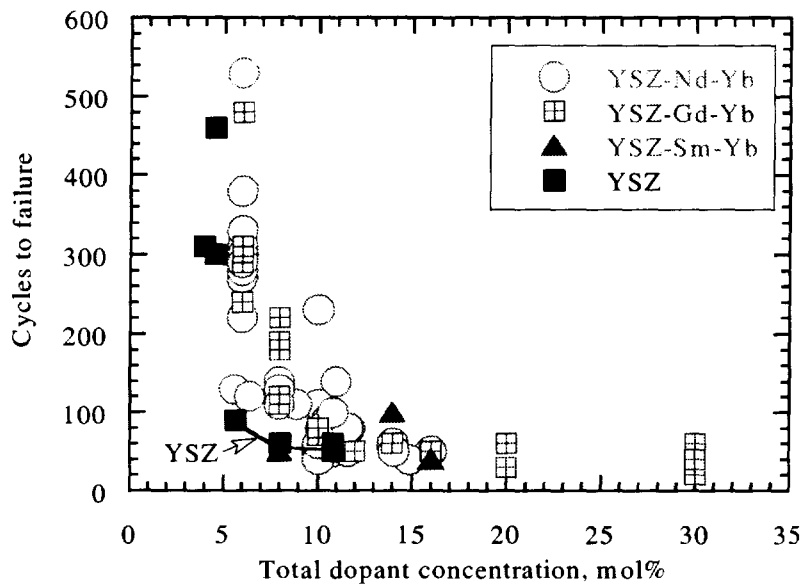
The intrinsic thermal conductivity of a ceramic coating is closely related to its lattice structure and lattice defects. The interactions between lattice phonon waves, and scattering of the lattice phonon and radiative photon waves by various length scale defects will greatly affect the thermal conductivity behavior [7]. As mentioned earlier, the multi-dopant oxides were incorporated into the  $ZrO_2$ - $Y_2O_3$  system by considering their interatomic and chemical potentials, lattice elastic strain energy (ionic size effect), polarization and electro-neutrality within the oxides [2]. The defect cluster design approach by the high stability, paired dopant oxides having distinctively different ionic sizes will effectively produce lattice distortion in the oxide solid solutions and facilitate local ionic segregation and thus defect clustering. Oxide defect clusters with appropriate sizes can effectively attenuate and scatter lattice phonon waves as well as radiative photon waves at a wide spectrum of frequencies. Therefore, by promoting the creation of thermodynamically stable, highly defective lattice structures with controlled defect cluster sizes, one can expect a reduced oxide intrinsic lattice and radiation thermal conductivity for these coatings.

The measured thermal conductivity for plasma-sprayed and EB-PVD thermal barrier coatings include both the contributions from the intrinsic coating conductivity and from the microstructural (such as coating porosity) effect. The coating thermal conductivity can be greatly reduced by the presence of microcracks and microporosity within the ceramic coatings. However, the conductivity reduction achieved by micro-porosity may not persist at high temperatures. The laser thermal conductivity test data for both the plasma-sprayed and EB-PVD thermal barrier coatings showed a significant coating conductivity increase with time. The increase in measured coating thermal conductivity has been attributed to ceramic sintering and densification [3, 4]. The advanced cluster oxide thermal barrier coatings showed reduced conductivity increase rates and thus improved sintering resistance due to the addition of the dopant oxides.

The added cluster dopant oxides can facilitate the formation of defective oxide lattice structures with essentially immobile defect clusters and/or nanoscale ordered phases, which improves the coating sintering resistance.



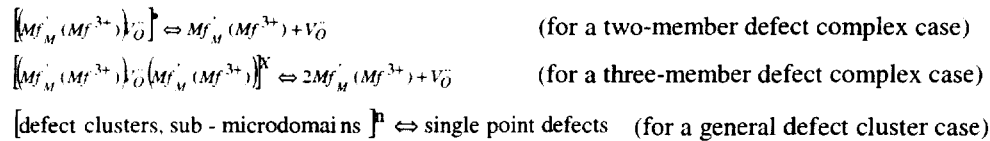
(a) Plasma-sprayed coatings



(b) EB-PVD coatings

Fig. 7 Furnace cyclic tests results for (a) plasma sprayed and (b) EB-PVD advanced cluster oxide coatings. The coating specimens were cyclic tested in a tubular or a box furnace at 1160°C with 45 min hot time cycles [6]. The coating cyclic life generally decreased with increasing the total dopant concentration. The multi-component cluster oxide coatings followed a similar trend as the YSZ coatings in the furnace cyclic behavior. However, the cluster coatings showed some promise to achieve significantly better cyclic lives than only yttria-doped zirconia coatings.

As exemplified for the ZrO<sub>2</sub> or HfO<sub>2</sub> based oxide systems, the following reactions describing the defect clustering and dissociation can be written according to Kröger-Vink notation [8]:



where  $(Mf_M^{\cdot} (Mf^{3+}))_O^{\cdot}$  is a valence defect for a dopant cation (valance +3) at the Zr (valence +4) site, and  $V_O^{\cdot}$  is the anion oxygen vacancy. Because the defect clusters are in dynamic equilibrium with the single point defects at high temperatures, the sophisticated oxide cluster design may suppress the cluster dissociation reactions at extremely high temperatures. By reducing the mobile defect concentrations through the defect clustering, the atomic (both cationic and anionic) mobility and mass transport within the oxides can be greatly reduced. This can explain why the cluster oxide thermal barrier coatings exhibited a lower conductivity rate of increase and thus the sintering resistance than the baseline YSZ coatings.

The thermal conductivity and the conductivity rate increase showed a clear minimum for the cluster oxide thermal barrier coatings at about 10 mol% total dopant concentration. This composition approximately corresponds to the phase boundary between the tetragonal phase zirconia (for the partially stabilized zirconia, *t* phase) and cubic phase zirconia at the testing temperatures. It is possible that the oxide defect clustering most extensive formation and development near this phase boundary, thus showing the maximum conductivity reductions and the minimum conductivity rates of increases. The sophisticated design approach will significantly improve the oxide sintering-creep resistance and other mechanical properties at high temperatures.

## CONCLUSIONS

Advanced multi-component, low conductivity oxide thermal barrier coatings have been developed based on an oxide-defect-clustering design approach and using a laser high heat flux thermal conductivity technique. The laser test approach emphasizes real-time monitoring of the coating conductivity at high temperatures in order to assess the overall coating thermal conductivity performance under engine-like heat flux and thermal gradient conditions.

The durability of the advanced low conductivity coatings was evaluated using cyclic furnace tests. Although the advanced cluster oxide coatings followed a similar trend as the ZrO<sub>2</sub>-Y<sub>2</sub>O<sub>3</sub> coatings in the furnace cyclic behavior where the coating cyclic life generally decreases with increasing the total dopant concentration, the cluster oxide coatings showed promise to achieve significantly better cyclic lives (cyclic lives comparable to that of zirconia-4.55mol%yttria) than the binary ZrO<sub>2</sub>-Y<sub>2</sub>O<sub>3</sub> coatings with equivalent dopant concentrations upon the further processing and dopant composition optimizations.

## REFERENCES

- [1] D. Zhu and R.A. Miller, "Defect Cluster Design Considerations in Advanced Thermal Barrier Coatings," NASA Glenn Research Center, Cleveland, Ohio, unpublished work 1999.
- [2] D. Zhu and R.A. Miller, "Low Conductivity and Sintering Resistant Thermal Barrier Coatings," US Patent Application Serial No. 09/904,084, USA.
- [3] D. Zhu and R.A. Miller, "Thermal Conductivity and Elastic Modulus Evolution of Thermal Barrier Coatings Under High Heat Flux Conditions," *Journal of Thermal Spray Technology*, vol. 9, pp. 175–180, 2000.
- [4] D. Zhu, R.A. Miller, B.A. Nagaraj, and R.W. Bruce, "Thermal Conductivity of EB-PVD Thermal Barrier Coatings Evaluated by a Steady-State Laser Heat Flux Technique," *Surface and Coatings Technology*, vol. 138, pp. 1–8, 2001.
- [5] D. Zhu, N.P. Bansal, K.N. Lee, and R.A. Miller, "Thermal Conductivity of Ceramic Thermal Barrier and Environmental Barrier Coating Materials," NASA Glenn Research Center, Cleveland NASA TM-211122, September 2001.
- [6] D. Zhu, J.A. Nesbitt, T.R. McCue, C.A. Barrett, and R.A. Miller, "Failure Mechanisms of Zirconia-Yttria Thermal Barrier Coatings," *Ceramic Eng. Sci. Proc.*, vol. 23, To be published, 2001.
- [7] P.G. Klemens and M. Gell, "Thermal Conductivity of Thermal Barrier Coatings," *Materials Science and Engineering*, vol. A245, pp. 143–149, 1998.
- [8] F.A. Kröger, *The Chemistry of Imperfect Crystals*. Amsterdam: North-Holland, 1964.

# REPORT DOCUMENTATION PAGE

*Form Approved*  
OMB No. 0704-0188

Public reporting burden for this collection of information is estimated to average 1 hour per response, including the time for reviewing instructions, searching existing data sources, gathering and maintaining the data needed, and completing and reviewing the collection of information. Send comments regarding this burden estimate or any other aspect of this collection of information, including suggestions for reducing this burden, to Washington Headquarters Services, Directorate for Information Operations and Reports, 1215 Jefferson Davis Highway, Suite 1204, Arlington, VA 22202-4302, and to the Office of Management and Budget, Paperwork Reduction Project (0704-0188), Washington, DC 20503.

|  |   |  |                                   |
|--|---|--|-----------------------------------|
| <b>1. AGENCY USE ONLY (Leave blank)</b>  | <b>2. REPORT DATE</b><br>May 2002                               | <b>3. REPORT TYPE AND DATES COVERED</b><br>Technical Memorandum                  |                                   |
| <b>4. TITLE AND SUBTITLE</b><br>Thermal Conductivity and Sintering Behavior of Advanced Thermal Barrier Coatings   |   | <b>5. FUNDING NUMBERS</b><br><br>WU-714-04-20-00                                 |                                   |
| <b>6. AUTHOR(S)</b><br><br>Dongming Zhu and Robert A. Miller   |   |  |                                   |
| <b>7. PERFORMING ORGANIZATION NAME(S) AND ADDRESS(ES)</b><br>National Aeronautics and Space Administration<br>John H. Glenn Research Center at Lewis Field<br>Cleveland, Ohio 44135-3191   |   | <b>8. PERFORMING ORGANIZATION REPORT NUMBER</b><br><br>E-13249                   |                                   |
| <b>9. SPONSORING/MONITORING AGENCY NAME(S) AND ADDRESS(ES)</b><br>National Aeronautics and Space Administration<br>Washington, DC 20546-0001   |   | <b>10. SPONSORING/MONITORING AGENCY REPORT NUMBER</b><br><br>NASA TM-2002-211481 |                                   |
| <b>11. SUPPLEMENTARY NOTES</b><br>Prepared for the 26th Annual International Conference on Advanced Ceramics and Composites sponsored by the American Ceramics Society, Cocoa Beach, Florida, January 13-18, 2002. Dongming Zhu, Ohio Aerospace Institute, 22800 Cedar Point Road, Brook Park, Ohio 44142; and Robert A. Miller, NASA Glenn Research Center. Responsible person, Dongming Zhu, organization code 5160, 216-433-5422.   |   |  |                                   |
| <b>12a. DISTRIBUTION/AVAILABILITY STATEMENT</b><br>Unclassified - Unlimited<br>Subject Categories: 24 and 27<br>Available electronically at <a href="http://gltrs.grc.nasa.gov/GLTRS">http://gltrs.grc.nasa.gov/GLTRS</a><br>This publication is available from the NASA Center for AeroSpace Information, 301-621-0390.   |   | <b>12b. DISTRIBUTION CODE</b><br><br>Distribution: Nonstandard                   |                                   |
| <b>13. ABSTRACT (Maximum 200 words)</b><br><br>Advanced thermal barrier coatings, having significantly reduced long-term thermal conductivities, are being developed using an approach that emphasizes real-time monitoring of thermal conductivity under conditions that are engine-like in terms of temperatures and heat fluxes. This is in contrast to the traditional approach where coatings are initially optimized in terms of furnace and burner rig durability with subsequent measurement in the as-processed or furnace-sintered condition. The present work establishes a laser high-heat-flux test as the basis for evaluating advanced plasma-sprayed and physical vapor-deposited thermal barrier coatings under the NASA Ultra Efficient Engine Technology (UEET) Program. The candidate coating materials for this program are novel thermal barrier coatings that are found to have significantly reduced thermal conductivities due to an oxide-defect-cluster design. Critical issues for designing advanced low conductivity coatings with improved coating durability are also discussed. |   |  |                                   |
| <b>14. SUBJECT TERMS</b><br>Thermal barrier coatings; Low thermal conductivity; Sintering; Thermal gradient testing  |   | <b>15. NUMBER OF PAGES</b><br>16   |                                   |
|  |   | <b>16. PRICE CODE</b>  |                                   |
| <b>17. SECURITY CLASSIFICATION OF REPORT</b><br>Unclassified   | <b>18. SECURITY CLASSIFICATION OF THIS PAGE</b><br>Unclassified | <b>19. SECURITY CLASSIFICATION OF ABSTRACT</b><br>Unclassified                   | <b>20. LIMITATION OF ABSTRACT</b> |